# Highly Selective Aptamer based Organic Electrochemical Biosensor with Pico-Level Detection

Nileshi Saraf, Eric R. Woods, Madison Peppler, Sudipta Seal

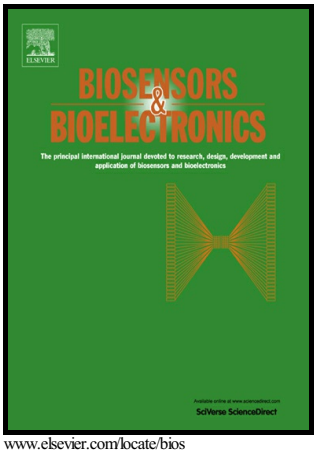


www.elsevier.com/locate/bios

PII: S0956-5663(18)30379-8
DOI: https://doi.org/10.1016/j.bios.2018.05.031
Reference: BIOS10489

To appear in: *Biosensors and Bioelectronic*

Received date: 21 March 2018
Revised date: 5 May 2018
Accepted date: 21 May 2018

Cite this article as: Nileshi Saraf, Eric R. Woods, Madison Peppler and Sudipta Seal, Highly Selective Aptamer based Organic Electrochemical Biosensor with Pico-Level Detection, *Biosensors and Bioelectronic,* https://doi.org/10.1016/j.bios.2018.05.031

# Highly Selective Aptamer based Organic Electrochemical Biosensor with Pico-Level Detection☆

Nileshi Saraf[a], Eric R. Woods[b1], Madison Peppler[c], Sudipta Seal[a,d*]

[a]*Advanced Materials Processing and Analysis Center, Department of Materials Science and Engineering, Nanoscience Technology Center, University of Central Florida, Orlando, FL.32826 USA.*
[b]*Cullen College of Engineering, University of Houston, Houston, Texas 77204 USA*
[c]*Department of Chemistry, University of Central Florida, Orlando, FL 32826.USA*
[d]*College of Medicine, University of Central Florida, Orlando, FL.32826 USA*

[*]Corresponding author. Tel.: +1-407823 5277. sudipta.seal@ucf.edu.



**Abstract**

An organic aptamer functionalized electrochemical transistor has been developed to detect the presence of epinephrine molecule which acts as an excitatory neurotransmitter. The abnormalities in the level of epinephrine are the direct symptoms of some diseases such as Takotsubo cardiomyopathy, myocardial infarction, arrhythmias and other heart related diseases. The present approach is based on immobilization of aptamers on the gate electrode which selectively binds to epinephrine with high affinity. The introduction of epinephrine in the system causes screening of negative charge of aptamers as well as the production of Faradaic current due to oxidation of epinephrine. The synergistic effect of these two events decreases the overall channel current which was seen in both transfer characteristics and current-time curve. Additional experiments against common interfering agents (dopamine, ascorbic acid, DOPAC etc) showed no decrease in the current which indicates high specificity of the sensor. Overall, the incorporation of aptamers in the transistor has allowed us to obtain a sensor exhibiting the lowest limit of detection for epinephrine (90 pM) till date which is comparable to normal physiological level. This approach provides a real-time detection of a large range of biomolecules and viral proteins in a time and cost-effective manner and has applications in point-of-care testing tool for several diagnostic applications.

Keywords: OECT, Aptamers, Epinephrine, PEDOT:PSS, point-of-care, Biosensor;

☆ Electronic supplementary information available
[1] UCF REU undergraduate

## 1. Introduction

Organic electrochemical transistors (OECTs) show great potential in the field of biosensors due to their low operating voltages and signal amplification. Over the past 30 years, OECTs have been utilized to detect numerous metal ions (Lin et al. 2010), small biomolecules (Kergoat et al. 2014; Tang et al. 2011a), proteins (Kubo and Eguchi 2015), oligonucleotides (Lin et al. 2011) and many other biological reagents (He et al. 2012; Tang et al. 2011b; Yang et al. 2009; Zhu et al. 2004). The cost effectiveness, availability, simplicity and portability of OECTs give them an edge over other traditional optical techniques used as biosensors in diagnosis (Aliakbarinodehi et al. 2017). The OECT device based on PEDOT: PSS (poly(3,4-ethylenedioxythiophene) polystyrene sulfonate) has shown a higher transconductance as compared to silicon based transistor and also outperformed electrolyte-gated graphene (Felderer and Fromherz 2011; Khodagholy et al. 2013a). PEDOT: PSS based OECTs offer a means of developing highly efficient point-of-care testing tool which exhibit high sensitivity and selectivity for the detection of molecule of interest.

A typical OECT device consists of a source-drain channel which is connected by an organic semiconducting material such as PEDOT: PSS as an active layer. The device can be switched on or off by varying the channel current that flows through the active layer controlled by an applied voltage from the third electrode called gate (Baker et al. 2006). The effective gate voltage depends on the potential difference between the PEDOT: PSS/electrolyte and gate/electrolyte interface. The conductivity of the active layer can be modulated through doping/de-doping effects of the electrochemical reactions occurring in the device (Lin and Yan 2012). Therefore, any charge transfer reaction which alters the surface potential of the gate electrode causes a significant change in channel current which can be measured with high accuracy using simple instrumentation (Ye and Yang 2014). The transducing properties along with high specificity in these devices make them excellent candidate in biosensing especially in healthcare industry where detection at an early stage can be extremely helpful.

The application of OECT device as a biosensor (He et al. 2012; Kergoat et al. 2014; Kubo and Eguchi 2015; Lin et al. 2011; Lin et al. 2010; Tang et al. 2011a; Tang et al. 2011b; Yang et al. 2009; Zhu et al. 2004) relies on the use of some biorecognition element such as enzymes, antibodies, oligonucleotides etc. which can transduce an electrochemical change in the presence of molecule of interest. Aptamers have been extensively used as the biorecognition molecule in the field of colorimetric (Saraf et al. 2017), (Zheng et al. 2011), electrochemical (Hansen et al. 2006), spectrophotometry (Zhou et al. 2014), (Lerga and O'Sullivan 2008), mass-sensitive (Song et al. 2008), and electrophoretic sensing (Mendonsa and Bowser 2004), (Turgeon et al. 2010). Aptamers are short DNA or RNA chains which selectively bind to a target molecule with high affinity. As compared to antibodies and enzymes, aptamers are resilient to heat, pH variation and chemically harsh conditions which makes them more efficient for practical applications (Kubo and Eguchi 2015). The process of SELEX (Systematic Evolution of Ligands by Exponential Enrichment) is used to design and select appropriate aptamers for the target molecules (Lin et al. 2011). Once the aptamers are designed, these can be synthesized in large quantities with high purity and reproducibility (Song et al. 2008). Thus, the use of aptamers offers a method for sensitive, selective, and affordable biomolecule detection.

In this study, an ultra-sensitive label free aptamer based OECT device has been developed to detect the presence of catecholamine epinephrine. Epinephrine, commonly known as Adrenaline, is responsible to prepare the body for "fight or flight" response by accelerating the heartbeat, stimulate glucose production (Rizza et al. 1979), dilate pupil (Thompson and Mensher 1971) etc. It is generally administered in case of severe emergency situations such as cardiac attack, anaphylactic shocks or asthma attacks. The physiological level of epinephrine in a human body under normal conditions ranges form 120-200 pM (Alpat et al. 2016) which shoots up in conditions like pulmonary edema (Worthen et al. 1969), Takotsubo cardiomyopathy (Akashi et al. 2008), myocardial infarction (Ferry et al. 1986), arrhythmias (Ajioka et al. 1986) and other thyroid problems (Alpat et al. 2016). Therefore, detection of epineprhine has significance in a variety of applications ranging from severe

allergy reactions, anti-doping regulations to treatments for cardiac attacks. The detetction of such small molecules has been done using various spectroscopic and chromatographic techniques (Carrera et al. 2007; Guan et al. 2000; Mak et al. 2015; Michałowski and Hałaburda 2001; Salmanpour et al. 2012; Saraf et al. 2017; Xu et al. 2012; Zhou et al. 2008) which has given impressive results, however these techniques are generally time consuming, complex and require skilled labour. The present approach introduces a highly efficient sensor providing a means for real-time detection in a timely and efficient manner and requires very small volume of the sample to run.

Figure 1A illustrates the aptamer based OECT device fabricated for the detection of epinephrine molecule in the present study. The gate, source, and drain electrodes are labelled as 1, 2, and 3 respectively. The source and drain electrodes are bridged by an organic semiconductor layer PEDOT: PSS, shown by the translucent, dark blue rectangle. The epinephrine specific aptamers are immobilized on to the gate electrode by thiol bonding. A PDMS mold is used to contain the electrolyte solution which ensures direct flow of current between the aptamer modified part of the gate (labelled as 4) and the PEDOT: PSS layer. The working principle of the current approach is based on the interaction of aptamers with epinephrine which enables the oxidation of the molecule in the vicinity of gate electrode. The oxidation generates $2e^-$ in the solution which produces Faradaic current in the device. The screening of the negative charge of aptamers along with the production of Faradaic current results in an increase in the effective gate voltage and decrease in the overall channel current which is measured as output signal. The present approach leads to a highly sensitive and specific label-free sensor which exhibits time and cost effectiveness, easy readout signals and utilizes off-the-shelf electronics.

## 2. Methods & Materials

### *2.1. Chemical Reagents*

Epinephrine binding thiolated 32-mer aptamers were synthesized and provided by BasePairBio Company (Pearland, TX). Chemicals such as epinephrine, 3,4-dihydroxyphenylacetic acid (DOPAC), tyrosine, glycine, dopamine, cysteine, L-ascorbic acid, tryptophan, PEDOT: PSS, and DMSO (dimethylsulfoxide) used during testing were purchased from Sigma-Aldrich (St. Louis, MZ). The TCEP (Tris (2-carboxyethyl) phosphine), Tris hydrochloride, phosphate buffered saline, and magnesium chloride that were utilized to make folding and resuspension buffers were also purchased from Sigma-Aldrich (St. Louis, MZ). LOR, Shipley microposit S1813, MF-CD-26 developer, and PG remover used for photolithography and pattering of the electrodes were purchased from Microchem (Westborough, MA). Gold pellets for deposition of gold electrodes were obtained from Kurt J. Lesker Company (Jefferson Hills, PA). The silicon wafers with orientation (100) were purchased from Wafer World Inc. (West Palm Beach, FL). For all experiments in the study, DNAse – RNAse free tips, vials and water purchased from Thermofisher (Waltham, MA), were used to avoid nuclease contamination.

### *2.2. Fabrication and measurement of OECT- based sensor*

The OECT device used in the present study (Figure 1A) was constructed on silicon wafers. After thorough cleaning of the wafers with acetone, isopropanol and ethanol, a 10-nm thick aluminium layer was deposited using Atomic Layer deposition to avoid any leakage current. The patterning on the Si wafer was done using LOR and Shipley as the photoresist and the sacrificial layer. The details of the photolithography are given in the supplementary information. The Ti/Au electrodes were deposited using AJA e-beam evaporator with a thickness of 50 nm for Au and 3 nm for Ti which acts as an adhesion layer. The entire channel length and the width of the electrodes were 2.6 cm and 0.5 cm respectively. The diameter of the gate electrode was kept at 0.4 cm.

The active layer of PEDOT: PSS was deposited using the same photolithography protocol. The solution of PEDOT: PSS was first filtered using a 0.22 µm membrane filter and modified with the addition of 5% by volume DMSO to decrease its solubility in aqueous solutions and increase its conductivity (Xia and Ouyang 2011). The filtered solution was spin coated onto the patterned wafer, followed by baking at 120°C for 40

minutes. The result was a thin, translucent layer of the active material deposited at the junction of the channel. The thickness of the layer as measured using Dektak Profilometer was around ~200 nm. The optimization of PEDOT: PSS deposition for uniform thickness, surface area and shape ensured consistent electrical and physical properties and less variability between different samples.

*2.3. Aptamer Preparation and Immobilization*

The lyophilized epinephrine binding aptamers were dissolved in suspension buffer (TE buffer, 0.1 mM EDTA, 10 mM Tris HCl, pH 7.5) to achieve a concentration of 100 µM. The aptamers were then aliquoted into smaller volumes and stored at -20°C for long term storage. To prepare the aptamers for conjugation, a standard protocol of folding and reducing steps was followed. The aptamers were diluted using the folding buffer (1 mM $MgCl_2$ and 0.01 M PBS, pH 7.5) to acquire the working concentration and incubated for 5 min at 95°C. The aptamers were then allowed to cool at room temperature for 15 min so that they can attain their folded conformation which enables binding to the analyte molecule. Before immobilization the aptamers were reduced using TCEP which cleaves the disulphide bonds and forms sulfhydryl group which is used for attachment to the gold surface. 10 µL of 10 µM reduced aptamers were applied to the gate electrode and allowed to incubate for 2 hours at room temperature. The excess aptamer solution was removed and the gate electrode was washed multiple times with PBS to remove any unbound aptamers from the surface.

*2.4. Testing Apparatus*

The electrical characteristics of the device were studied by a Keysight B2902A Precision Source and Measurement Unit controlled by EasyEXPERT software. The Keithley source meter was connected to the electrodes to apply and measure both voltage and current through the device simultaneously. During testing, a PDMS gel mold was used to contain the electrolyte solution between the aptamer modified part of the gate electrode and channel (Figure 1A, labelled as 4). The mold was shaped to ensure that the solution only contacted the PEDOT: PSS and the aptamer conjugated part of the gate electrode.

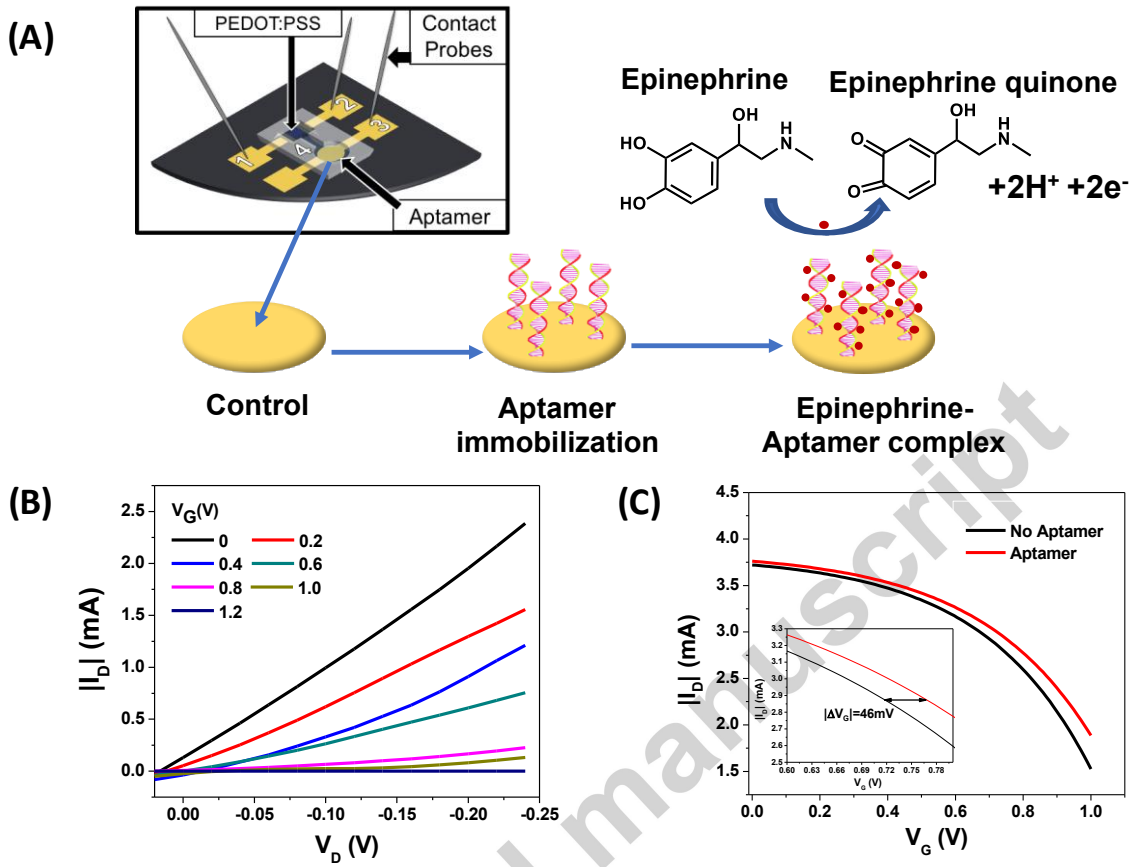


Fig 1: (A) Schematic illustration of the fabricated aptamer based OECT device on a silicon wafer. The source, drain and gate electrodes are labelled as 1, 2 and 3 respectively. Organic semiconducting layer of PEDOT: PSS is used as an active layer to bridge the channel and is represented by blue translucent rectangle. The magnified image of the gate electrode shows the immobilization of aptamers with help of thiol bonding. Further, the formation of epinephrine-aptamer complex upon addition of the epinephrine and the oxidation of epinephrine on the aptamer modified gate electrode has been shown. (B): Output characteristics ($I_D$ vs $V_D$) of the aptamer based OECT device measured in pure PBS solution in the absence of epinephrine at $V_G$ values of 0, 0.2, 0.4, 0.6, 0.8 and 1.0 V (from top to bottom). (C): Transfer characteristics ($I_D$ vs $V_G$) of the OECT device measured in PBS solution before and after immobilization of the aptamers on the gate electrode at $V_D$ = +0.1 V. The immobilization of the aptamers caused a right shift in the $V_G$ curve and the difference is measured out to be 46 mV.



## 3. Results

### *3.1. Output characteristics*

The output characteristics (Channel current, $I_D$ vs source-drain voltage, $V_D$) of the present OECT device at varying $V_G$ from 0 to +1.2 V along with a negative bias at $V_D$ is shown in Figure 1B. $I_D$ decreases with the increase in the gate voltage, $V_G$ which is a typical response of PEDOT: PSS based OECT device operating in depletion mode (increase gate voltage decreases the channel current) (Bernards and Malliaras 2007),

(Khodagholy et al. 2013b). The positive voltage applied at the gate induces cations from the electrolyte into PEDOT: PSS and compensate for the negative sulphonate anions present on PSS. This results in de-doping of the semiconducting layer causing a decrease in the hole density which in turn decreases the overall channel current. The de-doping in PEDOT: PSS is reversible in nature and the layer attains its original state when the gate voltage goes to zero (Bernards et al. 2008).

*3.2. Aptamer functionalization*

The functionalization of gate electrode with aptamers was confirmed by measuring the absorbance intensity of the applied aptamer solution before and after incubation. A significant decrease in absorbance intensity at 260 nm ($A_{260}$) was observed and quantitative analysis was done by plotting the calibration curve. The packing density for the attached aptamers was calculated to be $2.2 \times 10^{12}$ aptamers per $cm^2$. (Figure S1, Supplementary information). The higher packing density of the aptamers hinders the binding of aptamer-analyte due to the close packing of the strands whereas the lower packing density results in low performance because of the less binding sites available. The packing density of $2.2 \times 10^{12}$ lies near the optimum packing density ($1.6 \times 10^{12}$) as reported in the previous studies (Cheng et al. 2007; Zhang et al. 2018).

The effect of addition of aptamers over Au gate electrode was also examined through output characteristics. Figure 1C shows the $I_D$ versus $V_G$ characteristics at a $V_D$ of +0.1 V. The measurement was done in same electrolyte solution (pure PBS) before and after functionalization with epinephrine aptamers. A significant increase in channel current was observed after functionalization of gate electrodes. As reported previously, the performance of an OECT depends extensively on the surface potential and electrolyte/gate interface capacitance of the gate electrode (Khodagholy et al. 2013b; Yen et al. 2015; Zhang et al. 2015). Therefore, the immobilization of the aptamers over the gate electrode increased the overall negative charge density due to the presence of phosphate backbone which resulted in a decrease in the effective gate voltage and thus increase the overall channel current (Lin et al. 2011; Ohno et al. 2010; Tao et al. 2017).

*3.3. Transfer characteristics*

The transfer characteristics ($I_D$ vs $V_G$) were studied at $V_D$= +0.1V by using PBS as the electrolyte. The aptamers conjugated gate electrode of the device was incubated with epinephrine solution (90 pM, 900 pM, 9 nM, 90 nM, 900 nM, 9 µM, 90 µM, 900 µM) for 10 min and then washed off to remove unbound epinephrine. Figure 2A shows the channel current ($I_D$) vs. gate voltage ($V_G$) transfer curve at various concentrations of epinephrine. It was found that as the concentration of epinephrine increased from 90 pM to 900 µM, the transfer curve showed a distinct trend towards lower gate voltage. The change in gate voltage ($\Delta V_G$) as a function of concentration of epinephrine (log[Epi]) was plotted with the help of transfer characteristics ($I_D$ vs $V_G$) shown in Figure 2B. The device shows a constant increase in $|\Delta V_G|$ with increase in the concentration of epinephrine and a linear behavior can be seen from 90 pM to 900 nM. The $\Delta V_G$ becomes constant due to saturation of aptamer binding sites at higher concentration of epinephrine (>900 nM). The detection limit of the system was found to be 90 pM which showed a change of 53 mV upon addition of epinephrine.

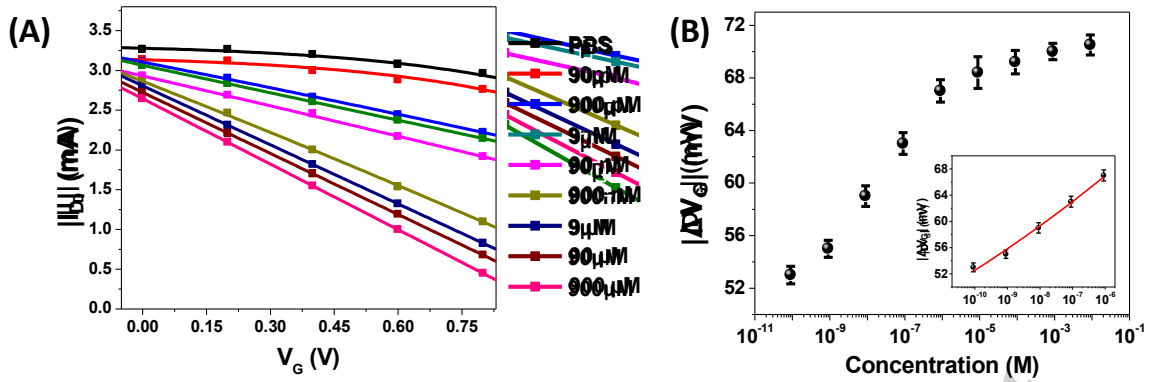


Fig 2:(A) Transfer characteristics ($I_D$ vs $V_G$) of the aptamer based OECT device in the presence of different concentration of epinephrine at $V_D$=+0.1V in PBS solution. A constant left shift in the $V_G$ with increasing amount of the epinephrine can be seen. (B) The change in $V_G$ of the OECT induced by interaction of epinephrine with the aptamers as derived by the transfer characteristics. The inset shows the fitting of the linear range (90 pM to 900 nM) having an $R^2$ value of 0.98.

*3.4. $I_D$ -time characteristics*

In order to monitor the real-time response of the aptamer modified OECT device, channel current, $I_D$ vs time curve was plotted at $V_D$= +0.1V and $V_G$= +0.7V as fixed parameters. The dependence of the source-drain current on the consecutive additions of epinephrine at various concentrations (90 pM-90 μM) is shown in Figure 3A. It can be seen that the addition of epinephrine at consecutive time intervals caused constant drops in the current which was seen almost immediately after the addition. It was also observed that along with the drop in current, there was slight increase in the channel current before the next addition. The binding of epinephrine to the aptamer is a dynamic process. The process includes constant association and dissociation of the molecules which takes a few seconds to equilibrate so that the system can attain lowest energy state. Therefore, instead of a straight curve, slight elevations were observed at lower concentrations (90 pM, 900 pM, 9 nM and 900 nM). At higher concentrations, sharp drop in the channel current was observed after the addition. The change in channel current ($|\Delta I_D|$) gives a linear dependence on logarithmic function of concentration of epinephrine as shown in Figure 3B.

*3.5. Selectivity Assay Results*

To test the selectivity of the aptamer based OECT sensor, an $I_D$ vs t test was conducted to observe the device response to biomolecules other than epinephrine. The interfering species selected were DOPAC, tryptophan, tyrosine, glycine, cysteine, dopamine, and ascorbic acid. These species were chosen either due to their structural similarity to epinephrine, or their similar biological functions. Figure 3C demonstrates device response in terms of change in $I_D$ with subsequent addition of interfering species at a time interval of 5 min. The sensor displayed a sharp decrease in $I_D$ after the addition of epinephrine whereas for other reagents, very slight/no change in the current was seen. The concentration of epinephrine used was 1 μM whereas 10 μM for the interfering species. The addition of cysteine and dopamine caused slight decrease in the current as can be observed at 22 min and 32 min. Interference from dopamine can be due to high structural similarity between epinephrine and dopamine. The thiol group present in the cysteine molecule could have interfered in the output signal as thiol is known to have a high affinity for the gold surface. Overall, the presence of aptamers suppressed the nonspecific binding of the interfering species at the gate electrode.

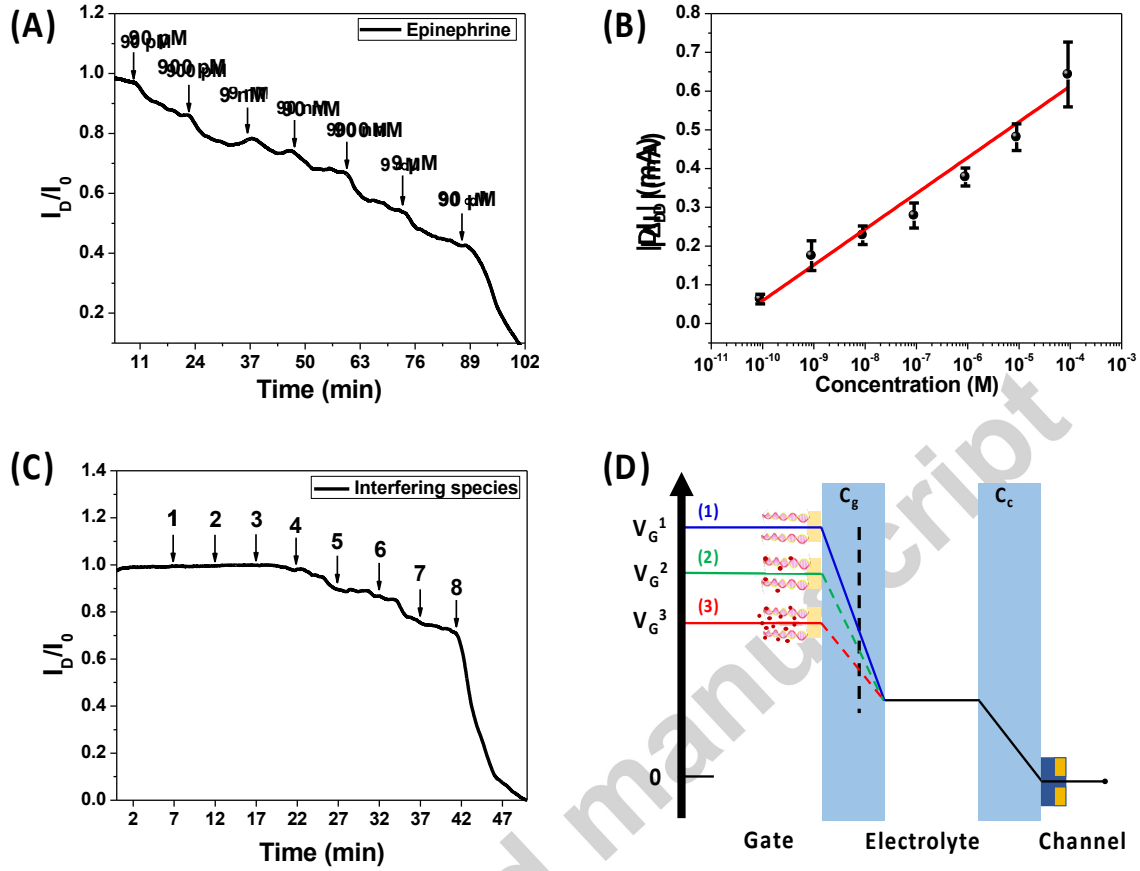


Fig 3: (A) The normalized time-current ($I_D/I_0$ versus t) characteristics of the present OECT device at $V_D$= +0.1 V and $V_G$= +0.7 V as fixed parameters. Addition of epinephrine was done at subsequent intervals of 13 minutes at a concentration of 90 pM, 900 pM, 9 nM, 90 nM, 900 nM, 9 µM, 90 µM - left to right. The increase in epinephrine resulted in constant drops in the channel current. (B) The change in channel current (mA) is plotted as a function of epinephrine concentration (90 pM-90 µM). A linear response was observed in the presence of epinephrine concentration with $R^2$ value of 0.96. Error bars represent the standard deviation from the mean value. The large error bar at 90 µM is due to the saturation of aptamer binding sites. (C) The normalized current response as a function of time ($I_D$ vs t) in the presence of interfering species (10 µM). The addition was done at an interval of 5 min in the order of DOPAC (1), tryptophan (2), tyrosine (3), dopamine (4), glycine (5), cysteine (6), ascorbic acid (7) and epinephrine (8). A sudden drop in the current was seen after the addition of epinephrine (1 µM). (D) A schematic illustration of the change in $V_G$ before and after addition of epinephrine. To maintain the same effective voltage in the device, the $V_G$ decreases to offset the Faradaic current produced due to the oxidation of epinephrine. $V_G^1$ represents the device with only immobilized aptamers and $V_G^2$, $V_G^3$ represents the new gate voltage with increasing concentration of epinephrine respectively. $V_G^1 > V_G^2 > V_G^3$

## 4. Discussions

The working of an OECT device depends largely on the change in conductance of the active layer due to the electrochemical doping/de-doping of the cations from the electrolyte controlled by variation in the effective gate voltage ($\Delta V_G^{eff}$) of the device. The $\Delta V_G^{eff}$ depends on the potential difference between the gate-

aptamer/electrolyte and PEDOT: PSS/electrolyte. In the present study, the $\Delta V_G^{eff}$ is dependent only on the change in the potential at gate-aptamer/electrolyte interface since epinephrine-aptamers complex are formed on the gate electrode. The channel current of an OCET device at a certain $V_G$ and $V_D$ is given by the following equation.

$$I_D = \frac{Wq\mu tp_0}{LV_P}\left(V_P - V_G^{eff} + \frac{V_D}{2}\right)V_D, (when\ |V_D| \ll \left|V_P - V_G^{eff}\right|) \quad (1)$$

$$V_P = \frac{qtp_0}{C_i}$$

$$V_G^{eff} = V_G + V_{offset} \quad (2)$$

where W and L represents the width and length of the channel, t is the thickness of the organic semiconductor layer (PEDOT: PSS), q is the electronic charge (1.6 x $10^{19}$), μ is the hole mobility, $C_i$ is the effective gate capacitance and $p_0$ is the initial hole density of the channel before applying $V_G$. $V_P$ is the pinch-off voltage and $V_D$ is the source-drain voltage. The $\Delta V_G^{eff}$ represents the effective gate voltage in the device and $V_{Offset}$ is the change in potential due to potential difference between the gate/electrolyte and PEDOT: PSS/electrolyte interface.

After the binding of epinephrine to the aptamers and application of positive voltage at the gate electrode, the electro-oxidation of epinephrine occurs. The oxidation causes release of 2*e*- in the solution which produces Faradaic current at the gate/electrolyte interface.

Epinephrine → Epinephrine quinone + $2H^+$ + $2e^-$

As a result, there is a decrease in the potential drop which increases the effective gate voltage of the device. This change in effective gate voltage further decreases the overall channel current as given in Eq 1. The change in effective gate voltage due to the electro-oxidation of epinephrine is given by:

$$V_{offset} = \frac{2.3(1+\gamma)kT}{ne}\log[Epi] + constant \quad (3)$$

where $\gamma$ is defined as the ratio between the capacitances of the channel ($C_C$) and the gate ($C_G$) with respect to the electrolyte, $\gamma$ = $C_C/C_G$; n (=2) is the number of electrons released during the oxidation, k and T represent the Boltzmann constant and room temperature and log[Epi] is the logarithmic function of concentration of epinephrine. As shown in Figure 2B, the slope of the fitted curve was found out to be 80 mV/decade in the linear region and thus the value of $\gamma$ was 1.24. The left shift in the $I_D$ vs $V_G$ curve with increase in the concentration of epinephrine, [Epi] is occurring due to the change in $V_{Offset}$ value which is directly proportional to the concentration of epinephrine as given in Eq 3. At higher concentrations of epinephrine, the $V_{Offset}$ becomes constant as the aptamer binding sites becomes saturated with epinephrine. The unbound epinephrine molecules were washed off before measuring the transfer characteristics. Therefore, the present sensor follows linear dependence on epinephrine concentration in the 90 pm-900 nM concentration regime.

Figure 3D represents the working of the present OECT device. As discussed previously, the immobilization of the aptamers introduces negative charge on the gate electrode which decreases the surface potential. To maintain the same effective voltage in the device, the $V_G$ increases and a shift in the transfer curve to the right side is observed (Figure 1C). However, upon the addition of epinephrine, the negative charge is balanced by the positively charged epinephrine ($pK_a$ 8.02), the overall effective gate voltage increases. To balance this extra potential change, the $V_G$ decreases and curve shifts to left side (Fig 2A). The change in $V_G$ showed a linear dependence on the concentration of the epinephrine molecule in the range of 90 pM to 900 nM after which it starts saturating. The synergistic effect of the binding event of aptamers along with the oxidation of the epinephrine molecule enhances the $\Delta V_G^{eff}$ as a function of concentration of epinephrine which amplifies the change in current and therefore the sensitivity of the present OECT device.

The addition of epinephrine on the bare gate electrode (no aptamers) was also studied with the help of real time $I_D$ response curve as shown in Figure S2 (supplementary information). The plot shows no change in the

current upon addition of epinephrine at 100 pM, 1 nM, 10 nM until 100 nM when a huge drop in current was observed. The decrease in the current is due to increased concentration of epinephrine in the electrolyte solution which facilitated the oxidation of epinephrine. The binding of epinephrine to the aptamers not only changes the surface potential of the gate electrode but also ensures the accumulation of epinephrine molecules in the vicinity of the gate electrode. The increased concentration of epinephrine around gate expedites the oxidation of the molecule and hence, maximizes the sensitivity of the sensor. Therefore, the presence of aptamers contributes to the high specificity of the sensor and also increases the detection limit by an order of atleast $10^3$ magnitude.

So far it has been established that the detection limit of the current approach is 90 pM. The physiological level of epinephrine for a healthy individual is in the range of 120-200 pM which increases in conditions like hyperthyroidism (359 ± 150 pM) and hypothyroidism (373 ± 150 pM) (Alpat et al. 2016). The increase in epinephrine level is also prominent in Takotsubo cardiomyopathy and Killip Class III myocardial infarction which averages the level to 6.9 nM and 2.1 nM after 1 or 2 days respectively (Wittstein et al. 2005). Quantitative analysis of epinephrine can be done using the present approach in the range of 90 pM to 900 nM which can be used for the early detection of pathological conditions as described above. Table 1 summarizes the different approaches used for the detection of epinephrine and their respective detection limits as listed in the literature. 2015 Mak *et al.* study reported a comparable detection limit of 100 pM (Mak et al. 2015) . The study is based on the electrical oxidation of epinephrine molecule using Pt based gate electrode modified with nafion and single walled carbon nanotube. The interference from ascorbic acid was seen at 100 nM whereas the present sensor showed no response to ascorbic acid even at a concentration of 10 µM. Selectivity is essential for real-world sensors to avoid the need for costly and time-consuming purification steps. Therefore, the aptamer-based OECT sensor presented in this work exhibits great potential in the real-world applications which gives fast and easy-to-read signals.

Table 1: Comparison of different techniques used for the detection of epinephrine and their respective detection limits.

| **Method** | **Detection limit** | **References** |
|---|---|---|
| Colorimetric | 900 pM | (Saraf et al. 2017) |
| Capillary Electrophoresis | 100 nM | (Xu et al. 2012) |
| Ion chromatography | 5.9 nM | (Guan et al. 2000) |
| HPLC-MS | 56 nM | (Carrera et al. 2007) |
| Differential Pulse Voltammetry | 90 nM | (Salmanpour et al. 2012) |
| Chemiluminescence | 1.1 µM | (Michałowski and Hałaburda 2001) |
| Differential Pulse Voltammetry | 30 nM | (Zhou et al. 2008) |
| OECT | 100 pM | (Mak et al. 2015) |
| OECT | 90 pM | Present method |

## Conclusions

A PEDOT: PSS based OECT sensor functionalized with aptamers was fabricated to detect the presence of epinephrine molecule. The high binding affinity of the aptamers towards epinephrine and the electro-oxidation of the molecule in the vicinity of gate electrode allow the present aptasensor with 90 pM limit of detection. The addition of epinephrine on the gate electrode resulted in a significant decrease in the channel current which was observed in both $I_D$ vs $V_G$ and $I_D$ vs time characteristics. In addition, experiments were conducted against common interfering agents to determine the selectivity of the OECT sensor. The device showed an instant drop in current upon addition of epinephrine as opposed to the other interfering molecules, indicating highly selective nature of the sensor. The inclusion of aptamers resulted in an increase of sensitivity by $10^3$ magnitude and high specificity towards epinephrine molecule. The present approach provides an easy, simple, rapid method for detecting epinephrine, however more work needs to be done in order to test the repeatability and reusability of the sensor. The future work will be aimed at extending the current approach to develop flexible sensor capable of

detecting various biomolecules by utilizing different aptamers on a single platform. The present work lays the ground for developing a wide range of personalized point-of-care testing tools for therapeutic applications.

**Acknowledgments**

The authors are thankful for the financial support from National Science foundation, Research Experiences for Undergraduates (NSF REU) program EEC- 1560007 and REU student E. Woods for his work. Authors are also thankful to Abraham Vazquez-Guardado, Nanoscience Technology Center, University of Central Florida for his help during fabrication of the samples.

**Conflicts of Interest**

There are no conflicts to declare.

**References**

Ajioka, M., Sugiyama, S., Ogawa, K., Satake, T., Ozawa, T., 1986. Mechanism of cardiac arrhythmias induced by epinephrine in dogs with hypokalemia. Journal of the American College of Cardiology 8(6), 1373-1379.
Akashi, Y.J., Goldstein, D.S., Barbaro, G., Ueyama, T., 2008. Takotsubo cardiomyopathy. Circulation 118(25), 2754-2762.
Aliakbarinodehi, N., Jolly, P., Bhalla, N., Miodek, A., De Micheli, G., Estrela, P., Carrara, S., 2017. Aptamer-based Field-Effect Biosensor for Tenofovir Detection. Scientific reports 7, 44409.
Alpat, Ş., Özdemir, K., Kılınç Alpat, S., 2016. Voltammetric Determination of Epinephrine in Pharmaceutical Sample with a Tyrosinase Nanobiosensor. Journal of Sensors 2016.
Baker, B.R., Lai, R.Y., Wood, M.S., Doctor, E.H., Heeger, A.J., Plaxco, K.W., 2006. An electronic, aptamer-based small-molecule sensor for the rapid, label-free detection of cocaine in adulterated samples and biological fluids. Journal of the American Chemical Society 128(10), 3138-3139.
Bernards, D.A., Macaya, D.J., Nikolou, M., DeFranco, J.A., Takamatsu, S., Malliaras, G.G., 2008. Enzymatic sensing with organic electrochemical transistors. Journal of Materials Chemistry 18(1), 116-120.
Bernards, D.A., Malliaras, G.G., 2007. Steady-State and Transient Behavior of Organic Electrochemical Transistors. Advanced Functional Materials 17(17), 3538-3544.
Carrera, V., Sabater, E., Vilanova, E., Sogorb, M.A., 2007. A simple and rapid HPLC–MS method for the simultaneous determination of epinephrine, norepinephrine, dopamine and 5-hydroxytryptamine: Application to the secretion of bovine chromaffin cell cultures. Journal of Chromatography B 847(2), 88-94.
Cheng, A.K., Ge, B., Yu, H.-Z., 2007. Aptamer-based biosensors for label-free voltammetric detection of lysozyme. Analytical chemistry 79(14), 5158-5164.
Felderer, F., Fromherz, P., 2011. Transistor needle chip for recording in brain tissue. Applied Physics A 104(1), 1.
Ferry, D.R., Henry, R.L., Kern, M.J., 1986. Epinephrine-induced myocardial infarction in a patient with angiographically normal coronary arteries. American heart journal 111(6), 1193-1195.
Guan, C., Ouyang, J., Li, Q., Liu, B., Baeyens, W., 2000. Simultaneous determination of catecholamines by ion chromatography with direct conductivity detection. Talanta 50(6), 1197-1203.

Hansen, J.A., Wang, J., Kawde, A.-N., Xiang, Y., Gothelf, K.V., Collins, G., 2006. Quantum-dot/aptamer-based ultrasensitive multi-analyte electrochemical biosensor. Journal of the American Chemical Society 128(7), 2228-2229.

He, R.-X., Zhang, M., Tan, F., Leung, P.H., Zhao, X.-Z., Chan, H.L., Yang, M., Yan, F., 2012. Detection of bacteria with organic electrochemical transistors. Journal of Materials Chemistry 22(41), 22072-22076.

Kergoat, L., Piro, B., Simon, D.T., Pham, M.C., Noël, V., Berggren, M., 2014. Detection of glutamate and acetylcholine with organic electrochemical transistors based on conducting polymer/platinum nanoparticle composites. Advanced Materials 26(32), 5658-5664.

Khodagholy, D., Rivnay, J., Sessolo, M., Gurfinkel, M., Leleux, P., Jimison, L.H., Stavrinidou, E., Herve, T., Sanaur, S., Owens, R.M., 2013a. High transconductance organic electrochemical transistors. Nature communications 4, 2133.

Khodagholy, D., Rivnay, J., Sessolo, M., Gurfinkel, M., Leleux, P., Jimison, L.H., Stavrinidou, E., Herve, T., Sanaur, S., Owens, R.M., 2013b. High transconductance organic electrochemical transistors. Nature communications 4.

Kubo, I., Eguchi, T., 2015. Study on Electrochemical Insulin Sensing Utilizing a DNA Aptamer-Immobilized Gold Electrode. Materials 8(8), 4710-4719.

Lerga, T.M., O'Sullivan, C.K., 2008. Rapid determination of total hardness in water using fluorescent molecular aptamer beacon. analytica chimica acta 610(1), 105-111.

Lin, P., Luo, X., Hsing, I., Yan, F., 2011. Organic electrochemical transistors integrated in flexible microfluidic systems and used for label-free DNA sensing. Advanced Materials 23(35), 4035-4040.

Lin, P., Yan, F., 2012. Organic thin-film transistors for chemical and biological sensing. Advanced materials 24(1), 34-51.

Lin, P., Yan, F., Chan, H.L., 2010. Ion-sensitive properties of organic electrochemical transistors. ACS applied materials & interfaces 2(6), 1637-1641.

Mak, C.H., Liao, C., Fu, Y., Zhang, M., Tang, C.Y., Tsang, Y.H., Chan, H.L., Yan, F., 2015. Highly-sensitive epinephrine sensors based on organic electrochemical transistors with carbon nanomaterial modified gate electrodes. Journal of Materials Chemistry C 3(25), 6532-6538.

Mendonsa, S.D., Bowser, M.T., 2004. In vitro evolution of functional DNA using capillary electrophoresis. Journal of the American Chemical Society 126(1), 20-21.

Michałowski, J., Hałaburda, P., 2001. Flow-injection chemiluminescence determination of epinephrine in pharmaceutical preparations using raw apple juice as enzyme source. Talanta 55(6), 1165-1171.

Ohno, Y., Maehashi, K., Matsumoto, K., 2010. Label-free biosensors based on aptamer-modified graphene field-effect transistors. Journal of the American Chemical Society 132(51), 18012-18013.

Rizza, R., Haymond, M., Cryer, P., Gerich, J., 1979. Differential effects of epinephrine on glucose production and disposal in man. American Journal of Physiology-Endocrinology And Metabolism 237(4), E356.

Salmanpour, S., Tavana, T., Pahlavan, A., Khalilzadeh, M.A., Ensafi, A.A., Karimi-Maleh, H., Beitollahi, H., Kowsari, E., Zareyee, D., 2012. Voltammetric determination of norepinephrine in the presence of acetaminophen using a novel ionic liquid/multiwall carbon nanotubes paste electrode. Materials Science and Engineering: C 32(7), 1912-1918.

Saraf, N., Bosak, A., Willenberg, A., Das, S., Willenberg, B.J., Seal, S., 2017. Colorimetric detection of epinephrine using an optimized paper-based aptasensor. RSC Advances 7(77), 49133-49143.

Song, S., Wang, L., Li, J., Fan, C., Zhao, J., 2008. Aptamer-based biosensors. TrAC Trends in Analytical Chemistry 27(2), 108-117.

Tang, H., Lin, P., Chan, H.L., Yan, F., 2011a. Highly sensitive dopamine biosensors based on organic electrochemical transistors. Biosensors and Bioelectronics 26(11), 4559-4563.

Tang, H., Yan, F., Lin, P., Xu, J., Chan, H.L., 2011b. Highly sensitive glucose biosensors based on organic electrochemical transistors using platinum gate electrodes modified with enzyme and nanomaterials. Advanced Functional Materials 21(12), 2264-2272.

Tao, W., Lin, P., Hu, J., Ke, S., Song, J., Zeng, X., 2017. A sensitive DNA sensor based on an organic electrochemical transistor using a peptide nucleic acid-modified nanoporous gold gate electrode. RSC Advances 7(82), 52118-52124.
Thompson, H.S., Mensher, J.H., 1971. Adrenergic mydriasis in Horner's syndrome: Hydroxyamphetamine test for diagnosis of postganglionic defects. American journal of ophthalmology 72(2), 472-480.
Turgeon, R.T., Fonslow, B.R., Jing, M., Bowser, M.T., 2010. Measuring aptamer equilibria using gradient micro free flow electrophoresis. Analytical chemistry 82(9), 3636-3641.
Worthen, M., Placik, B., Argano, B., MacCanon, D., Luisada, A., 1969. On the mechanism of epinephrine-induced pulmonary edema. Japanese heart journal 10(2), 133-141.
Xia, Y., Ouyang, J., 2011. PEDOT: PSS films with significantly enhanced conductivities induced by preferential solvation with cosolvents and their application in polymer photovoltaic cells. Journal of Materials Chemistry 21(13), 4927-4936.
Xu, X., Zhang, H., Shi, H., Ma, C., Cong, B., Kang, W., 2012. Determination of three major catecholamines in human urine by capillary zone electrophoresis with chemiluminescence detection. Analytical biochemistry 427(1), 10-17.
Yang, S.Y., DeFranco, J.A., Sylvester, Y.A., Gobert, T.J., Macaya, D.J., Owens, R.M., Malliaras, G.G., 2009. Integration of a surface-directed microfluidic system with an organic electrochemical transistor array for multi-analyte biosensors. Lab on a Chip 9(5), 704-708.
Ye, W., Yang, M., 2014. A Functionalized Nanoporous Alumina Membrane Electrochemical Sensor for DNA Detection with Gold Nanoparticle Amplification. Advances in Bioceramics and Biotechnologies II: Ceramic Transactions 247, 191.
Yen, C.-W., de Puig, H., Tam, J.O., Gómez-Márquez, J., Bosch, I., Hamad-Schifferli, K., Gehrke, L., 2015. Multicolored silver nanoparticles for multiplexed disease diagnostics: distinguishing dengue, yellow fever, and Ebola viruses. Lab on a Chip 15(7), 1638-1641.
Zhang, L., Wang, G., Wu, D., Xiong, C., Zheng, L., Ding, Y., Lu, H., Zhang, G., Qiu, L., 2018. Highly selective and sensitive sensor based on an organic electrochemical transistor for the detection of ascorbic acid. Biosensors and Bioelectronics 100, 235-241.
Zhang, S., Kumar, P., Nouas, A.S., Fontaine, L., Tang, H., Cicoira, F., 2015. Solvent-induced changes in PEDOT: PSS films for organic electrochemical transistors. APL materials 3(1), 014911.
Zheng, Y., Wang, Y., Yang, X., 2011. Aptamer-based colorimetric biosensing of dopamine using unmodified gold nanoparticles. Sensors and Actuators B: Chemical 156(1), 95-99.
Zhou, M., Guo, L.-P., Hou, Y., Peng, X.-J., 2008. Immobilization of Nafion-ordered mesoporous carbon on a glassy carbon electrode: Application to the detection of epinephrine. Electrochimica Acta 53(12), 4176-4184.
Zhou, N., Zhang, J., Tian, Y., 2014. Aptamer-based spectrophotometric detection of kanamycin in milk. Analytical Methods 6(5), 1569-1574.
Zhu, Z.-T., Mabeck, J.T., Zhu, C., Cady, N.C., Batt, C.A., Malliaras, G.G., 2004. A simple poly (3, 4-ethylene dioxythiophene)/poly (styrene sulfonic acid) transistor for glucose sensing at neutral pH. Chemical Communications(13), 1556-1557.

Highlights

- Epinephrine biosensor developed using aptamer functionalized transistor
- Decrease in current in transfer and time-current curve upon addition of epinephrine
- Specificity test against common interfering species showed no decrease in current
- Aptamer inclusion resulted in $10^3$ times sensitivity and high specificity
- Lowest detection limit (90 pM) was achieved using the present technique